Global Change Biology

Global Change Biology (2011) **17**, 410–424, doi: 10.1111/j.1365-2486.2010.02269.x

Differential responses of production and respiration to temperature and moisture drive the carbon balance across a climatic gradient in New Mexico

KRISTINA J. ANDERSON-TEIXEIRA*†, JOHN P. DELONG*‡, ANDREW M. FOX*, DANIEL A. BRESE* and MARCY E. LITVAK*

*University of New Mexico, Albuquerque, NM 87131, USA, †University of Illinois at Urbana-Champaign, Urbana, IL 61801, USA, ‡Department of Ecology and Evolutionary Biology, Yale University; New Haven, CT 06520, USA

Abstract

Southwestern North America faces an imminent transition to a warmer, more arid climate, and it is critical to understand how these changes will affect the carbon balance of southwest ecosystems. In order to test our hypothesis that differential responses of production and respiration to temperature and moisture shape the carbon balance across a range of spatio-temporal scales, we quantified net ecosystem exchange (NEE) of CO_2 and carbon storage across the New Mexico Elevational Gradient, which consists of six eddy-covariance sites representing biomes ranging from desert to subalpine conifer forest. Within sites, hotter and drier conditions were associated with an increasing advantage of respiration relative to production such that daily carbon uptake peaked at intermediate temperatures – with carbon release often occurring on the hottest days – and increased with soil moisture. Across sites, biotic adaptations modified but did not override the dominant effects of climate. Carbon uptake increased with decreasing temperature and increasing precipitation across the elevational gradient; NEE ranged from a source of $\sim 30\,g\,C\,m^{-2}\,yr^{-1}$ in the desert grassland to a sink of $\sim 350\,g\,C\,m^{-2}\,yr^{-1}$ in the subalpine conifer forest. Total aboveground carbon storage increased dramatically with elevation, ranging from $186\,g\,C\,m^{-2}$ in the desert grassland to $26\,600\,g\,C\,m^{-2}$ in the subalpine conifer forest. These results make sense in the context of global patterns in NEE and biomass storage, and support that increasing temperature and decreasing moisture shift the carbon balance of ecosystems in favor of respiration, such that the potential for ecosystems to sequester and store carbon is reduced under hot and/or dry conditions. This implies that projected climate change will trigger a substantial net release of carbon in these New Mexico ecosystems (~ 3 Gt CO_2 statewide by the end of the century), thereby acting as a positive feedback to climate change.

Keywords: biomass, climate change, eddy-covariance, elevational gradient, net ecosystem exchange, precipitation, semiarid ecosystems, southwest North America

Received 14 January 2010 and accepted 3 May 2010

Introduction

Climate change will fundamentally alter the structure and dynamics of many ecosystems (IPCC, 2007). Responses of carbon flux and storage are particularly consequential, as any net change in an ecosystem's carbon balance acts as a feedback to climate change (e.g., Field *et al*., 2007). The most pervasive mechanism by which climate change stands to alter carbon storage in terrestrial ecosystems is by shifting the balance between CO_2 uptake through gross primary production (GPP) and release through ecosystem respiration (R_{eco}), thereby altering the net ecosystem exchange (NEE) of CO_2 (e.g., Ciais *et al*., 2005; Piao *et al*., 2008; Piao *et al*., 2009). Predicting the response of NEE to climate change remains a challenge because NEE varies far less predictably with climate than either GPP or R_{eco}, whose strong responses to both temperature and water availability largely cancel (e.g., Law *et al*., 2002; Luyssaert *et al*., 2007; Reichstein *et al*., 2007; Yuan *et al*., 2009). There are, however, differences in how GPP and R_{eco} respond to climate, and these differences are key to understanding how climate affects NEE. In this study, we draw upon existing concepts of how differential responses of GPP and R_{eco} to temperature and moisture drive NEE to understand how temperature and moisture shape the carbon balance of semiarid ecosystems at spatio-temporal scales ranging from day-to-day variation within ecosystems to annual carbon flux and storage across a broad climatic gradient. This provides a basis for understanding how the carbon balance of semiarid ecosystems in Southwestern North America

Correspondence: Marcy E. Litvak, e-mail: mlitvak@unm.edu

will respond to the predicted imminent transition to a warmer, more arid climate with more severe droughts (Leung *et al*., 2004; Christensen *et al*., 2007; Seager *et al*., 2007; Weiss *et al*., 2009).

NEE is driven by differential responses of GPP and whole-R_{eco} to climatic conditions. Over short temporal scales, these responses and their physiological drivers are clearly defined; however, they become more complex across longer time scales, as R_{eco} is highly dependent upon GPP (Hogberg *et al*., 2001; Ryan & Law, 2005; Stoy *et al*., 2008). Specifically, autotrophic respiration is regulated such that it typically consumes $<60\%$ of production on daily time scales (Gifford, 1994) and $<75\%$ on annual time scales (DeLucia *et al*., 2007; Litton *et al*., 2007). Heterotrophic respiration (primarily from mycorrhizal fungi and soil microbes) is likewise constrained by carbon inputs through roots or litterfall (e.g., Hogberg *et al*., 2001), such that – over sufficient time scales in steady state ecosystems – R_{eco}/GPP is necessarily constrained at or below 1. A shift in climatic conditions, however, can disrupt this balance, resulting in altered patterns of carbon uptake or release (e.g., Randerson *et al*., 1999; Ciais *et al*., 2005; Monson *et al*., 2006; Arnone *et al*., 2008; Piao *et al*., 2008; Piao *et al*., 2009; Schwalm *et al*., 2009; Hu *et al*., 2010). Over larger spatio-temporal scales (i.e., across sites or over temporal scales where the community has had time to adjust to climatic conditions), the effects of climate on the carbon balance are moderated by adaptations of species within the communities and other abiotic site characteristics (e.g., soils), with physiological traits modifying but not overriding the biophysical constraints imposed by climate.

Production and respiration respond differently to temperature (in the absence of water limitation). On a physiological level, respiration in both plants and heterotrophs responds more strongly to temperature than does photosynthesis (Kirschbaum, 1995; Allen *et al*., 2005). As a result, the ratio R_{eco}/GPP increases with temperature such that both plants and whole ecosystems tend to release carbon in response to sudden increases in temperature (e.g., Rustad *et al*., 2001; Atkin *et al*., 2007). However, providing that the higher temperatures are not far outside the range typically experienced by plants, autotrophic respiration rapidly acclimates to temperature to maintain homeostasis with photosynthate supply (Atkin & Tjoelker, 2003; King *et al*., 2006). Heterotrophic respiration is limited by carbon inputs; although the temperature sensitivity of respiration remains relatively constant across seasons, reference respiration (i.e., respiration at a certain temperature) varies seasonally with carbon inputs (e.g., Groenendijk *et al*., 2009). Changing temperatures perturb this balance. For example, fall warming in northern ecosystems differentially favors respiration over production, resulting in carbon losses, while spring warming has the opposite effect (Randerson *et al*., 1999; Piao *et al*., 2008; Piao *et al*., 2009). Over longer spatio-temporal scales, the relationship of NEE to temperature on regional to global scales is often fairly ambiguous (e.g., Luyssaert *et al*., 2007; Reichstein *et al*., 2007), being confounded by factors such as stand age, N deposition, CO_2 fertilization, and other nonequilibrium dynamics (Gifford, 1994; Magnani *et al*., 2007; Piao *et al*., 2009).

In terms of water availability, production benefits more from higher levels of soil moisture than does R_{eco}. Specifically, autotrophic respiration responds less strongly to moisture than does GPP (Atkin & Macherel, 2009), as evidenced by the fact that plants are able to gain carbon under favorable moisture conditions, but burn carbon stores (and eventually die) under protracted water stress (e.g., Adams *et al*., 2009; Breshears *et al*., 2009). Likewise, compared with GPP, heterotrophic respiration responds to lower levels of soil moisture – but increases less strongly with increasing moisture, as microbes can operate at lower water potentials than most plants and can escape harsh conditions in suitable microsites (Orchard & Cook, 1983; Foster, 1988). Although heterotrophic respiration responds more rapidly and to lower levels of soil moisture (i.e., the pulse response; e.g., Huxman *et al*., 2004b; Jenerette *et al*., 2008; Inglima *et al*., 2009), it generally loses its advantage as moisture increases (Austin, 2002), and sustained increases in water availability generally favor production. Thus, in water-limited environments, carbon uptake typically increases with increasing water availability (e.g., Huxman *et al*., 2004a, b; Muldavin *et al*., 2008). In contrast, because production responds with more sensitivity to drought than does respiration (Schwalm *et al*., 2009), water-limited ecosystems often lose carbon during a drought (e.g., Ciais *et al*., 2005; Arnone *et al*., 2008; Schwalm *et al*., 2009), and these effects may persist beyond the drought because of damage to canopy function (Reichstein *et al*., 2002; Arnone *et al*., 2008). Over longer spatio-temporal scales where communities are adapted to climatic conditions, both individual plants and whole ecosystems struggle to maintain a favorable carbon balance under dry conditions, but are able to sequester substantial amounts of carbon when moisture is abundant.

In semiarid ecosystems, where water stress and temperature tend to be positively correlated, the differential effects of temperature and moisture availability on production and respiration will tend to work in the same direction. That is, hot and dry conditions inhibit the accumulation of significant carbon stocks, whereas cooler and wetter conditions strongly favor GPP over R_{eco}, resulting in carbon buildup. These differential

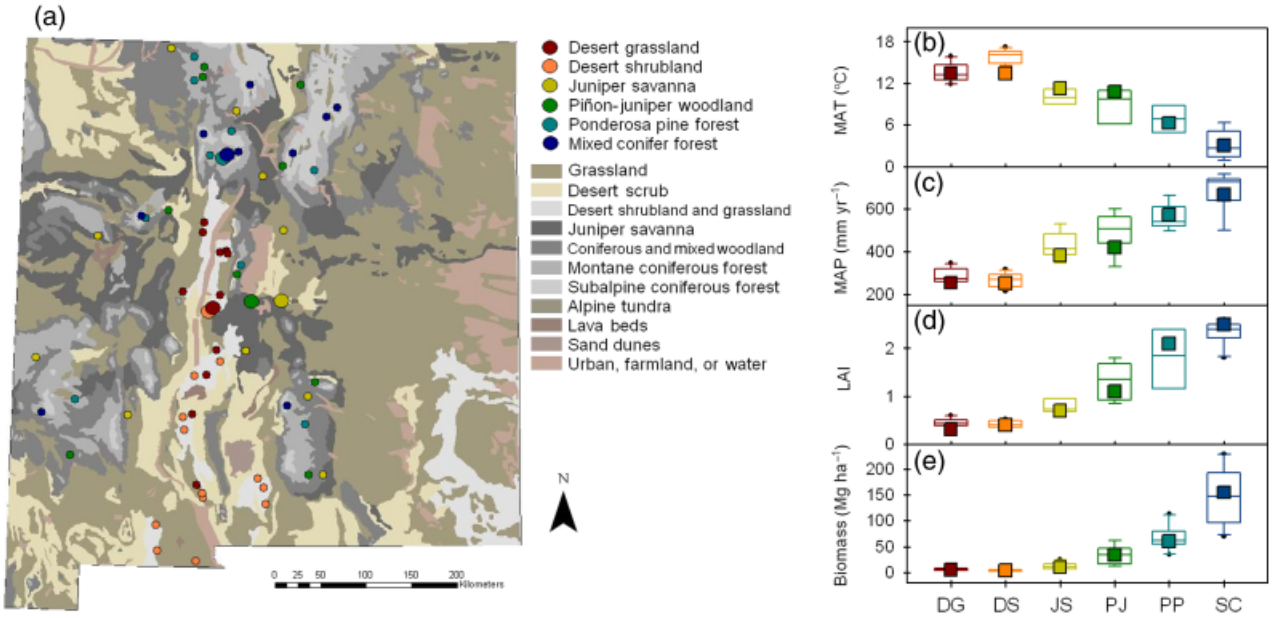

Fig. 1 Representation of New Mexican ecosystems in the New Mexico Elevational Gradient (NMEG). (a) Location of NMEG sites and auxiliary sites in relation to the statewide distribution of biomes, as classified by Dick-Peddie (1999). Auxiliary sites are used to evaluate the represenativeness of NMEG sites in terms of (b) mean annual temperature (MAT), (c) mean annual precipitation (MAP), (d) leaf area index (LAI) from MODIS, and (e) aboveground biomass. Boxplots indicate the median (center line), first and third quartiles (box edges), data range (whiskers), and outliers (black dots) of the auxiliary site data. NMEG sites are indicated by solid squares.

responses will define the responses of ecosystems to climate change, which is expected to bring hotter, more arid conditions to southwestern North America (Leung *et al*., 2004; Christensen *et al*., 2007; Seager *et al*., 2007; Weiss *et al*., 2009). Indeed, climate change is already evident. Records indicate increasing temperatures in the southwest (Portmann *et al*., 2009). While a long-term trend in precipitation is less clear (Portmann *et al*., 2009), the region has recently experienced severe drought, the frequency and intensity of which is likely to increase (e.g., Hughes & Diaz, 2008). In the face of these changes, it is critical to understand how carbon flux and storage respond to climate in southwest ecosystems.

Here, we examine how differential responses of production and respiration to temperature and water availability shape the carbon balance of semiarid ecosystems at a range of spatio-temporal scales across the New Mexico Elevational Gradient (NMEG; Fig. 1, Table 1), which consists of six sites representing major biomes and instrumented with eddy-covariance systems. Typical of semiarid regions, conditions range from hot and arid at low elevations to cool and mesic at high elevations. This gradient is ideal for understanding the response of carbon flux and storage to climate, as both temperature and precipitation vary markedly across elevations and through time. Environmental gradients such as this provide a powerful means of understanding the fundamental mechanisms through which climate shapes ecosystems (e.g., Whittaker & Niering, 1975; Austin, 2002; Anderson-Teixeira *et al*., 2008). They are also useful for predicting potential effects of climate change. Long-term responses of ecosystems to climate change can be difficult to predict based on field experiments, as transitional dynamics may differ from those of the eventual steady state. Comparisons of 'steady-state' ecosystems across environmental gradients reveal how climate shapes ecosystems over long time scales, and are therefore invaluable in complementing experimental studies to predict the effects of climate change (e.g., Shaver *et al*., 2000; Rustad *et al*., 2001).

We use data on carbon flux and storage across the NMEG to test three hypotheses regarding the fundamental mechanisms through which climate shapes semiarid ecosystems. First, we predict that at each site, GPP and R_{eco} will respond differentially to temperature and soil moisture, such that daily carbon uptake is highest at intermediate temperatures and under moist conditions. Second, both within and across sites, daily R_{eco}/GPP will increase with temperature and decrease with increasing soil moisture, indicating that adaptations modify but do not override the dominant effects of climatic constraints. Third, across sites, carbon uptake will increase with elevation in response to decreasing temperature and increasing moisture, both of which favor production over respiration. As a result, the long-term carbon balance, as reflected in living and

Table 1 Characteristics of the New Mexico Elevational Gradient sites

Site	Location	Latitude, longitude	Elevation (m)	Mean annual temp. (°C)	Measured mean annual temp. (°C)	Mean annual precip. (mm yr^{-1})	Measured annual precip. (mm yr^{-1})	USDA soil type	Dominant species	Biome Area in New Mexico (million ha)
Desert grassland (DG)	Sevilleta LTER	34.34N, 106.73W	1596	13.4	13.3 (2007); 13.0 (2008)	244	253 (2007); 309 (2008)	Loamy sand	*Bouteloua eriopoda*, *Gutierrezia sarothrae*, *Ceratoides lanata*	5.52
Desert shrubland (DS)	Sevilleta LTER	34.35N, 106.69W	1605	13.4	14.3 (2007); 14.0 (2008)	244	200 (2007); 267 (2008)	Very gravelly sandy loam	*Larrea tridentata*, *G. sarothrae*	1.86
Juniper savannah (JS)	7-Up 7-Down Ranch (private)	34.43N, 105.86W	1926	11.2	11.8 (2008)	369	389 (2008)	Fine sandy loam	*Juniperus monosperma*, *Bouteloua gracilis*	3.11
Piñon juniper woodland (PJ)	Deer Canyon Preserve (private)	34.36N, 106.27W	2126	10.8	10.1 (2008)	420	336 (2008)	Loam	*Pinus edulis*, *J. monosperma*	4.20
Ponderosa pine forest (PP)	Valles Caldera National Preserve	35.86N, 106.60W	2486	6.3	6.7 (2007); 6.4 (2008)	550	731 (2007); 656 (2008)	Silt loam	*Pinus ponderosa*, *Quercus gambelii*	2.41
Subalpine conifer forest (SC)	Valles Caldera National Preserve	35.89N, 106.53W	3049	3.1	5.2 (2007); 4.9 (2008)	667	864 (2007); 737 (2008)	Coarse sandy loam	*Picea engelmannii*, *Picea pugens*, *Abies lasiocarpa var. lasiocarpa*, *Abies concolor*	0.90

LTER, Long Term Ecological Research; temp., temperature.

nonliving carbon pools, will increase with elevation. All three of these hypotheses imply a potential loss of carbon uptake and storage under hotter and drier conditions. In order to investigate the potential effects of climate change, we conclude with an analysis of how the NM carbon balance would change based on the climate responses observed here.

Materials and methods

Site descriptions

The NMEG consists of six sites in central New Mexico, each representing a biome that is common throughout the state: desert grassland (DG), desert shrubland (DS), juniper savannah (JS), piñon-juniper woodland (PJ), ponderosa pine forest (PP), and subalpine conifer forest (SC) (Fig. 1, Table 1). All sites were located on well-drained soils with low (<25%) clay content (data from National Resources Conservation Service, 2009). None of the sites experienced any major disturbances for >30 years before or during the 2-year measurement period (2007–2008). Known disturbance histories include grazing at DG and DS sites until 1973, light seasonal cattle grazing at the JS site, and in the PP and SC region, logging before 1972, and grazing of cattle (1800s to 1999) and a historically large elk herd (1960s to present). All of these disturbances are fairly typical for these biomes in New Mexico, and are unlikely to systematically bias patterns observed across the gradient.

The NMEG is distributed along a strong gradient in both temperature and precipitation. According to data obtained from DAYMET for years 1980–2003 (Oak Ridge National Laboratory, Distributed Active Archive Center; http://www.daymet.org/default.jsp), mean annual precipitation (MAP) ranges across the gradient from 244 mm yr^{-1} at the desert sites to 667 mm yr^{-1} at the subalpine conifer site, and mean annual temperature (MAT) ranges from 13 °C at the desert sites to 3 °C at the subalpine conifer site. Precipitation is dominated by a bimodal seasonal cycle consisting of deep penetrating snow/rainfall during the winter and subtropical 'monsoon' systems that deliver sporadic heavy rainfall during the summer. The proportion of annual precipitation contributed by the monsoon decreases with elevation; in 2007–2008, monsoon precipitation contributed 66%, 70%, 53%, 45%, 46%, and 36% of total precipitation in DG, DS, JS, PJ, PP, and SC sites, respectively. Measured precipitation and temperature for 2007–2008 did not differ substantially from long-term averages (Table 1).

To ensure that the sites are typical examples of biomes that they represent, we compared tower site long-term climate data, remotely sensed leaf area index (LAI) estimates, and biomass estimates to these variables from ten auxiliary sites of each biome type (Fig. 1). Auxiliary sites of each biome type were identified based on the USDA forest inventory analysis for forests (USDA Forest Service) and vegetation range maps (Dick-Peddie, 1999) for desert grassland and shrubland. Homogeneity of vegetation and terrain over a 1 km area was verified using aerial photographs from Google Earth® and the MOD15A2 product [Oak Ridge National Laboratory Distributed Active Archive Center (ORNL DAAC), 2009]. Climate data was obtained from DAYMET (see above). LAI for a 1 km area centered on each site was obtained from the Oak Ridge National Laboratory Distributed Active Archive Center (ORNL DAAC). Specifically, we averaged the maximum annual value obtained from the MOD15A2 product for the years 2000–2007 (ORNL DAAC, 2009). For forests, aboveground biomass estimates were obtained from the USDA forest inventory analysis (USDA Forest Service, 2007). For the tower sites, if estimates were not available, we selected nearby inventory plots of similar elevation and climate within a 1–3 km radius (matches were generally close). Biomass data for desert grassland and shrubland sites was obtained from transect sampling at the Jornada (auxiliary sites; $n = 3$; Jornada LTER, 2007) and Sevilleta (representing tower sites) LTERs (Sevilleta LTER, 2007). This analysis revealed that the NMEG sites are representative of their biome types; specifically, with respect to all four variables considered (i.e., MAT, MAP, biomass, and LAI), the tower sites were within the same range as other sites of their type (Fig. 1).

Micrometeorological measurements

Direct, continuous measurements of surface carbon dioxide, water, and energy were made in all six tower sites using tower-mounted eddy covariance systems. Four of the towers (in desert grassland, shrubland, ponderosa pine, and mixed conifer sites) were operational in Jan 2007. The juniper savanna and piñon-juniper systems were installed in May 2007 and November 2007, respectively. The eddy covariance instrumentation and processing of all fluxes was identical in all six sites. Covariances were obtained from 10 Hz measurements of vertical wind speed and gas concentration using three-axis sonic anemometers (CSAT-3, Campbell Scientific, Logan, UT, USA) and open-path gas analyzers (LI-7500, LiCor, Lincoln, NB, USA), respectively, controlled by Campbell Scientific CR5000 dataloggers. Additional instrumentation at each site measured net radiation (CNR1 Kipp & Zonen, Bohemia, NY, USA), air temperature and relative humidity (HMP45C Vaisala, Helsinki, Finland), photosynthetically active radiation (Licor SZ190), precipitation (Campbell Scientific TE525MM-L), soil temperature (107 probes, Campbell Scientific), and soil water content (SWC, Campbell Scientific CS 616) in four to six profiles per site. SWC measurements used here are at 30–40 cm depth.

Half-hourly averages of the covariances were computed and corrected for density fluctuations due to temperature and water vapor using the WPL procedure (Webb *et al*., 1980) and frequency response using the method of Massman (2000). We used the planar fit coordinate system applied to 30-min averages of the covariances to correct for anemometer tilt with respect to the terrain.

Eddy covariance underestimates nocturnal NEE when inversions, low turbulence and advection prevent CO_2 generated by the ecosystem from being detected by eddy covariance systems. A friction velocity (u^*) filter was used to reject data obtained when turbulence was low (u^* less than a threshold value). Data gaps created by the u^* filter, malfunctioning instruments, and when rain were filled using data from nearby

days with similar meteorological conditions following the methodology of Falge *et al*. (2001) and Reichstein *et al*. (2005). NEE was partitioned into R_{eco} and GPP using the methodology of Reichstein *et al*. (2005); exponential relationships of nighttime R_{eco} to temperature for 10-day time windows were used to predict daytime R_{eco}, and GPP was calculated as R_{eco}-NEE (Flanagan *et al*., 2002). Half-hourly values of NEE, R_{eco}, and GPP were summed to obtain daily and annual totals. Flux uncertainties associated with random error were calculated using methodology similar to that of Hollinger & Richardson (2005). Systematic uncertainty represents a far larger source of error with the eddy-covariance technique; however, this type of error remains difficult to quantify.

Biometric measurements

We measured aboveground biomass of all plants, woody debris, and litter during the summers of 2007 (DG, DS, JS, PP, and SC) and 2008 (PJ). The sampling setup was designed to characterize the portions of the site contributing most strongly to the eddy-covariance measurements. Specifically, at each site, we established an 80 m transect out from the tower in the direction of the prevailing winds and two 40 m transects at right angles to this. Four large circular plots were centered at 35 and 70 m from the tower along the long transect and at 35 m from the tower on each 40 m transect. Sampling radii were selected to include, on average, at least 20 individuals of the dominant woody species (5 m in DS, 17.5 m in JS, and 10 m in all other sites).

Aboveground herbaceous biomass ($g\,m^{-2}$) was destructively harvested every 10 m along each transect ($n = 16$). For sites dominated by woody vegetation (all but grassland), measurements were taken in both in both under-canopy and open positions located as close as possible to the transect points. Within a 0.5×0.5 m (DG) or 1×1 m quadrat (other sites), we determined the density of C_4 grasses, C_3 grasses, forbs, cacti, and conifer seedlings. We then clipped all non-woody vegetation at ground level and sorted each type into living and dead material. Samples were dried to constant weight at 60 °C and weighed. Biomass estimates were weighted according to percent canopy cover.

For each large circular plot ($n = 4$), total aboveground biomass and foliage biomass of both live and dead woody plants ($g\,m^{-2}$) were estimated based on allometries (Table S1). For shrubs and succulents, we measured height, the greatest diameter, and the perpendicular diameter. Masses were estimated using volume-based allometries calculated using data from the Sevilleta LTER (Muldavin, 2004; Allen *et al*., 2008), Arizona (Enquist & Niklas, 2002), or a general biomass–foliage mass allometry (West *et al*., 1999). For juniper, we measured height, two perpendicular diameters, and root collar diameter – i.e., trunk diameter at ground level or, when multiple stems were present, an equivalent diameter (Grier *et al*., 1992). Biomass was estimated using allometries developed in northern Arizona (Grier *et al*., 1992), which appear to provide reasonable estimates for trees in New Mexico (E. A. Yepez, personal communication). For all other trees, we measured dbh and height. Aboveground biomass was estimated using general allometries developed for US tree species (Jenkins *et al*., 2003), and foliar biomass was estimated using general allometries (Jenkins *et al*., 2003) or, when available, locally collected allometric data (McDowell *et al*., 2008b). For saplings, we measured height. In most cases, allometries for saplings were not available, so we estimated biomass by extrapolating the allometric height–biomass relationship observed for larger trees. Some biomass estimates could only be obtained through extrapolation of allometries beyond the size range for which they were developed; however, the mathematical behavior of all allometries was carefully examined to ensure that they were biologically reasonable and matched the behavior of more general allometries (West *et al*., 1999; Enquist & Niklas, 2002). For all woody plants, we estimated percent dead or missing foliage, and subtracted this percent from live foliage biomass estimates.

Coarse woody debris (CWD), which was defined as any dead, detached aboveground wood at least 3 cm in diameter and 1 m in length, was measured in each large circular plot. For logs and branches, we recorded length, the diameter at each end, and the estimated percent missing (decayed). Volume was calculated using the formula for volume of a truncated cone and converted to mass using estimates of wood-specific gravity (Jenkins *et al*., 2003). For relatively intact, fallen dead trees, we estimated mass as with standing trees.

Fine woody debris, which we defined as any dead wood smaller than CWD and >40 cm length (smaller pieces were counted as litter), was sampled in $1\,m^2$ quadrats every 20 m along each transect ($n = 8$). As with herbaceous biomass, separate measurements were made in under-canopy and open-space positions and weighted according to percent canopy cover. Diameter and length were recorded, and volume was estimated using the formula for the volume of a cylinder. As with CWD, volume was converted to mass using the wood-specific gravities (Jenkins *et al*., 2003).

Litter was collected from 40 cm diameter rings every 10 m along each transect ($n = 16$). Samples were divided between under-canopy and open-space positions and weighted according to percent canopy cover. Samples were dried to constant weight at 60 °C and weighed. All organic matter estimates ($g\,dry\,m^{-2}$) were converted to units of carbon ($g\,C\,m^{-2}$) assuming a biomass carbon content of 50%.

The soil organic matter fraction in the top 10 cm of mineral soil ($g\,SOM\,g^{-1}$ soil) was measured using 12–18 replicate cores (2.5 cm diameter), subsamples of which were ashed to determine organic matter content (R. L. Sinsabaugh, T. Adamson, & M. E. Litvak, unpublished results). This was converted to total soil organic carbon (SOC) in the top 10 cm ($g\,C\,m^{-2}$) based on measurements of soil bulk density ($g\,soil\,cm^{-3}$) and the assumption that soil organic matter is 58% carbon by weight.

Data analysis

For analyses of responses of daily NEE, R_{eco}, and GPP to temperature and SWC, we removed data for a 2-day period following rain events. We then used linear regression (type III S.S. ANOVA) to evaluate the separate and combined effects of temperature and SWC on NEE. SWC values were

ln-transformed to account for their strongly right-skewed distribution and because CO_2 fluxes respond nonlinearly to changes in SWC. For analyses of the separate effects of SWC, we included only data for the months in which growth was not inhibited by low temperatures. For each site, this period was defined based on the temperature threshold above which 80% of annual GPP occurs. Months in which average temperature exceed this threshold were as follows: DG: June–September, DS: April–September, JS: March–October, PJ: March–October, PP: April–October, SC: May–October. For analyses of the relationship of daily R_{eco}/GPP to temperature and SWC, values were binned by 1 °C increments and into 30 logarithmically spaced SWC bins, respectively. Bins with $n<4$ were excluded. We used ANOVA (type III SS) to evaluate the relationship of ln(R_{eco}/GPP) to temperature or ln(SWC), site, and the interaction term. In addition to this across site analysis, we evaluated these relationships within each site. Because the SWC record for the PJ site did not begin until August 2008, we included 2009 data for this site for within-site analyses of flux responses to SWC. MAT and total precipitation in 2009 were very similar to those of 2008 at this site [MAT: 10.1 (2008), 10.6 (2009); precipitation: 336 mm (2008), 329 mm (2009)].

For cross-site analyses of the relationships between ecosystem properties (i.e., annual NEE, annual R_{eco}/GPP, and carbon storage) and climatic variables (measured MAT and annual precipitation for fluxes; long-term averages for carbon storage), we tested linear, exponential, logarithmic, and power fits to determine the best fits (Table S3). For NEE and R_{eco}/GPP, where four sites (DG, DS, PP, SC) had 2 years of data, we included year as a covariate. MAP and MAT displayed a strong negative correlation ($R^2 = 97\%$ for long-term climatic averages; $R^2 = 92\%$ for measured annual values), such that variation in ecosystem properties across the gradient was – from a statistical standpoint – approximately equally well-explained by either one.

Data for global comparison

We assembled data on annual NEE (g C m^{-2} yr^{-1}) for unmanaged ecosystems (forests and nonforests) with no known recent disturbance. Micrometeorological estimates of net annual CO_2 flux from the ecosystem to the atmosphere were obtained from the AmeriFlux (AmeriFlux Network) and FLUXnet (Falge *et al*., 2005) online databases (accessed February 2009), from a recent compilation of global forest data (Luyssaert *et al*., 2007), and from peer-reviewed publications (ISI search keywords: carbon flux, NEE, eddy-covariance; Risser *et al*., 1981; Valentini *et al*., 1995; Clark *et al*., 1999; Dugas *et al*., 1999; Flanagan *et al*., 2002; Santos *et al*., 2003; Suyker *et al*., 2003; Novick *et al*., 2004; Veenendaal *et al*., 2004; Gilmanov *et al*., 2005; Leuning *et al*., 2005; Gilmanov *et al*., 2006; Beringer *et al*., 2007; Svejcar *et al*., 2008; Wohlfahrt *et al*., 2008). Estimates were based on complete 1-year period with gap filling by the artificial neural network method (AmeriFlux data), nonlinear regression with *u** correction (FLUXnet data), or the methodologies used by individual publications. Data on forest biomass was obtained from a recent review (Keith *et al*., 2009). We included only sites with estimates for both live aboveground biomass and CWD, which were summed to attain aboveground carbon storage (g C m^{-2}).

Results

As predicted, within sites, GPP and R_{eco} responded differentially to temperature and soil moisture, resulting in systematic variation in NEE with these variables (Figs 2–3). Specifically, at all six sites, both GPP and R_{eco} increased with temperature, often peaking and declining at the highest temperatures (Fig. 2). Within all sites, GPP exhibited a substantial advantage over respiration at low temperatures; however, R_{eco} matched or exceeded GPP at the highest temperatures (Fig. 2). As a result, daily carbon uptake was always highest at intermediate temperatures, with sink strength peaking near 20 °C in the desert sites and 5–10 °C at the higher elevations.

During the months in which growth was not inhibited by low temperatures, SWC (30–40 cm depth) influenced daily carbon flux at all sites (Fig. 3). At the three lowest sites, both GPP and R_{eco} increased strongly with SWC, whereas these fluxes were less strongly influenced by SWC in the higher elevation sites. In all sites, differential responses of R_{eco} and GPP resulted in a significant decline in NEE (sign convention: negative indicates uptake by the ecosystem) with ln(SWC) ($P<0.02$).

The observed responses of NEE to temperature and SWC (Figs 2–3) were similar when these variables were considered in combination. For periods when growth was not inhibited by low temperatures, an ANOVA including both temperature and ln(SWC) (no interaction term) revealed that the effects of temperature were consistently positive (i.e., increased temperatures favoring respiration) in all sites ($P<0.0001$) but the desert grassland, where the relationship was not significant ($P=0.31$). NEE consistently decreased with increasing SWC ($P<0.0001$ in all sites but the piñon-juniper, where $P=0.23$). The interactive effects of temperature and SWC were significant in three sites: the desert grassland (−interaction; $P<0.002$), desert shrubland (+interaction; $P<0.009$), and subalpine conifer forest (−interaction; $P=0.05$).

Over the entire year, the effects of temperature on NEE were positive in two sites (JS and PJ; $P<0.001$), not significant in three (DG, DS, and PP; $P>0.05$), and negative in one (MC; $P<0.001$). The inconsistency in responses in year-round data is attributable to the nonlinear nature of the NEE–temperature relationship (Fig. 2). NEE decreased significantly with SWC in all sites ($P<0.006$) except for the desert shrubland, where the response was not significant ($P=0.13$). There were

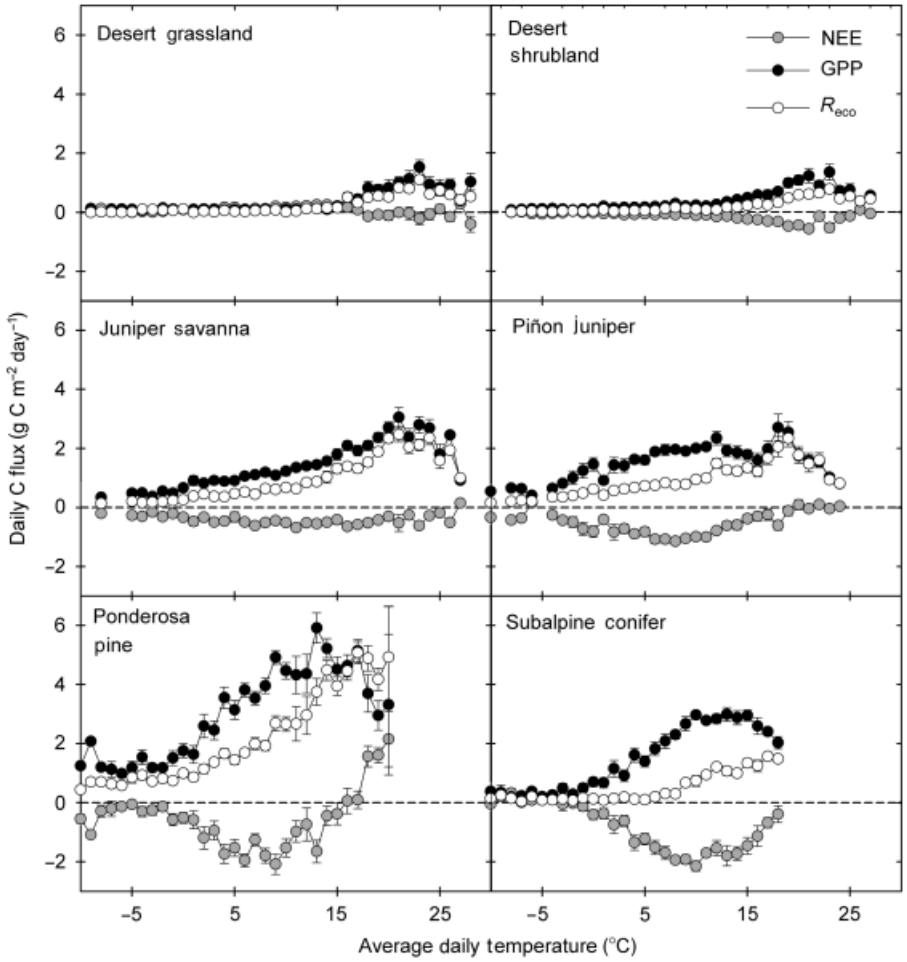

Fig. 2 Daily carbon dioxide fluxes – GPP, R_{eco}, and NEE – over the entire year as a function of mean daily temperature across the NMEG. For illustrative purposes, data are binned into 1 °C intervals. Plotted are the mean ± 1 SE for each bin. GPP, gross primary production; R_{eco}, release through ecosystem respiration; NEE, net ecosystem exchange; NMEG, New Mexico Elevational Gradient.

significant negative interactive effects of temperature and SWC at four sites (DG, PJ, PP, SC; all $P \leq 0.002$).

Both within and across sites, daily R_{eco}/GPP increased with temperature and decreased with increasing soil moisture (Fig. 4). Specifically, R_{eco}/GPP increased exponentially with temperature both within sites (significant at $P < 0.0001$ for all sites but DG, where $P = 0.15$) and across sites ($P < 0.001$; Fig. 4a). An ANOVA (type III S.S.) analysis revealed that ln(R_{eco}/GPP) is influenced most strongly by temperature ($F = 167.5$, $P < 0.0001$), but also by site ($F = 32.1$, $P < 0.0001$) and the site × temperature interaction ($F = 8.3$, $P < 0.0001$). Similarly, R_{eco}/GPP decreased as a power function with SWC within half the sites ($P < 0.05$) and across all sites ($P = 0.002$; Fig. 4b). In an ANOVA (type III S.S.) including site as a covariate, ln(R_{eco}/GPP) was strongly influenced by site ($F = 5.9$, $P < 0.001$) and the site × ln(SWC) interaction ($F = 4.9$, $P = 0.001$), whereas the effects of ln(SWC) alone were not significant ($F = 2.2$, $P = 0.14$).

These effects played out on annual time scales such that NEE decreased with increasing elevation on annual time scales (Fig. 5a; Table S3). Specifically, NEE ranged from a small source of 35–50 g C m^{-2} yr^{-1} at the desert grassland to a substantial sink of 344–355 g C m^{-2} yr^{-1} at the mixed conifer forest. Across the elevational gradient, sink strength was reduced by 33 ± 5 g C m^{-2} yr^{-1} per degree increase in measured MAT ($P < 0.001$), or by 0.5 ± 0.1 g C m^{-2} yr^{-1} for every 1 mm yr^{-1} decrease in annual precipitation ($P < 0.001$). NEE did not differ significantly between 2007 and 2008 ($P > 0.3$).

Partitioning of NEE into GPP and R_{eco} revealed that both of these fluxes increased with elevation, peaked at the ponderosa pine forest and decreased to the mixed

conifer forest (Fig. 5b). However, GPP was increasingly favored over R_{eco} in the cooler and moister conditions associated with high elevations; the fraction of annual production released as respiration (R_{eco}/GPP) decreased with increasing elevation ($P = 0.01$), ranging from 1.3 to 1.5 in the desert grassland to 0.32 −0.36 in the subalpine conifer forest.

Living and nonliving carbon pools, which reflect the long-term carbon balance, increased dramatically with elevation (Fig. 6; Table S2–S3). Live foliage biomass – including both herbaceous and woody components – increased linearly with increasing MAP/decreasing MAT ($P < 0.01$). Live aboveground biomass – including plants of all size classes – displayed an accelerating increase with elevation (Fig. 6). This relationship was best fit by a linear function for MAP ($P = 0.001$) and a lognormal relationship for MAT ($P < 0.001$). Likewise, nonliving organic material – including standing dead plants, woody debris, and litter – increased as a power function of increasing MAP ($P = 0.002$) or a logarithmic function of decreasing MAT ($P = 0.004$). All together, the total aboveground organic material increased dramatically with increasing MAP/decreasing MAT, ranging from $186 \pm 17\,g\,C\,m^{-2}$ in the desert grassland to $26\,600 \pm 1710\,g\,C\,m^{-2}$ in the mixed conifer forest. This relationship was best described as a power function of MAP ($P < 0.001$) or a logarithmic function of MAT ($P < 0.001$). Soil organic carbon in the top 10 cm of mineral soil likewise increased as a power function of increasing MAP ($P = 0.001$) or a logarithmic function of decreasing MAT ($P = 0.002$).

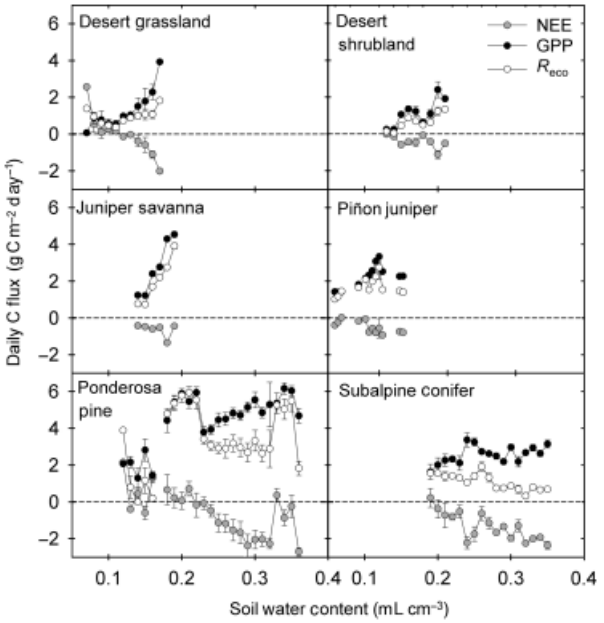

Fig. 3 Daily carbon dioxide fluxes – GPP, R_{eco}, and NEE – as a function of mean daily soil water content (30–40 cm depth) during periods when growth is not inhibited by low temperatures for all six sites across the NMEG. For illustrative purposes, data are binned into 30 logarithmically spaced bins. Plotted are the mean ± 1 SE for each bin. GPP, gross primary production; R_{eco}, release through ecosystem respiration; NEE, net ecosystem exchange; NMEG, New Mexico Elevational Gradient.

Discussion

Across the NMEG, differential effects of temperature and water availability on production and respiration shape the carbon balance over a range of spatio-temporal scales. Within each site, GPP and R_{eco} respond differently to temperature and SWC (alone or in combination), and NEE responds as the difference between

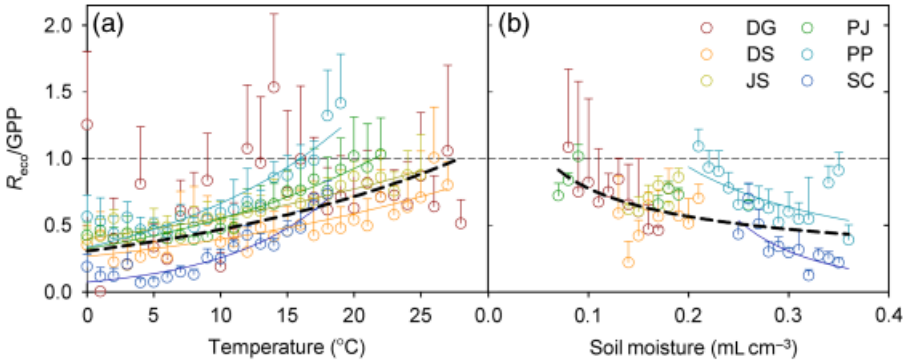

Fig. 4 Relative advantage of daily respiration over production (R_{eco}/GPP) as a function of (a) air temperature and (b) soil moisture (30–40 cm depth; months where low temperatures do not limit growth) for all six sites across the NMEG. Colored lines represent significant ($P < 0.05$) within-site relationships, and dashed black lines represent the average response across sites ($P < 0.005$ for both). GPP, gross primary production; R_{eco}, release through ecosystem respiration; NMEG, New Mexico Elevational Gradient; DG, desert grassland; DS, desert shrubland; JS, juniper savannah; PJ, piñon-juniper woodland; PP, ponderosa pine forest; SC, subalpine conifer forest.

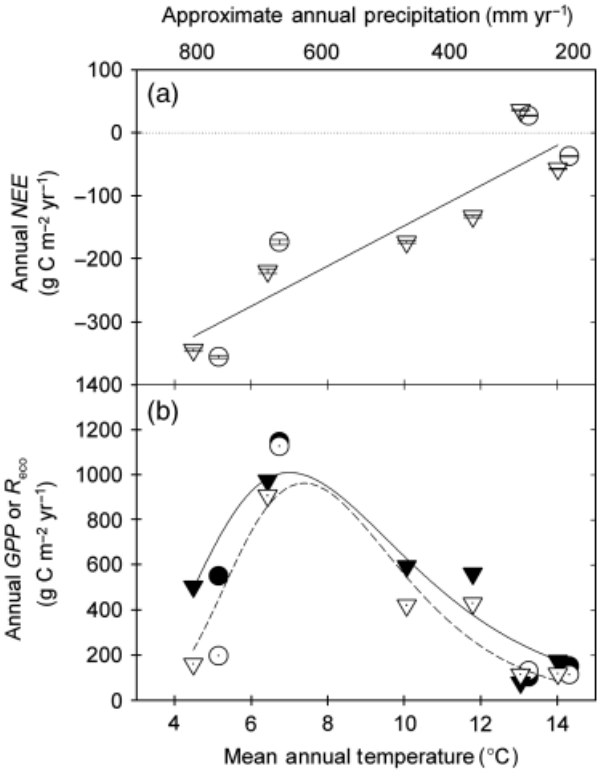

Fig. 5 Annual carbon fluxes as a function of mean annual temperature across the NMEG in 2007 (circles) and 2008 (squares): (a) annual NEE (sign convention-negative indicates carbon sink; error bars characterize random error only and represent 1 SD) and (b) annual GPP (solid symbols) and R_{eco} (hollow symbols). Measured annual precipitation was closely correlated to temperature across the gradient ($R^2 = 92\%$), and is also represented on the *x*-axis. Curves (solid: NEE, GPP; dashed: R_{eco}) are fit to 2008 data. GPP, gross primary production; R_{eco}, release through ecosystem respiration; NEE, net ecosystem exchange; NMEG, New Mexico Elevational Gradient.

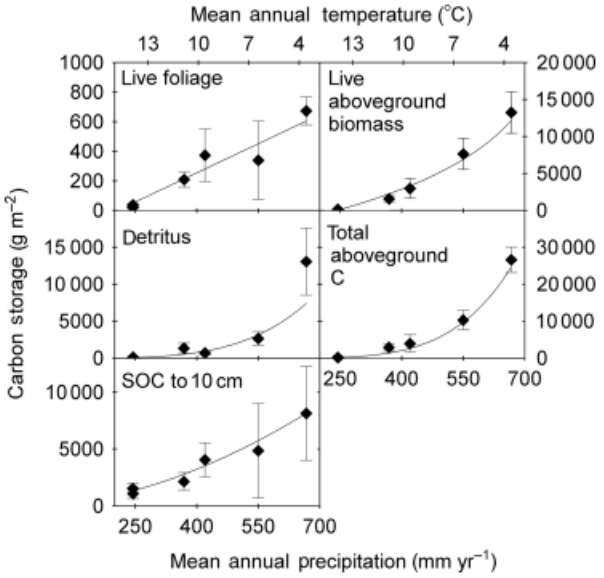

Fig. 6 Aboveground storage of carbon (mean ± 2 SE) in live foliage, live biomass, nonliving organic matter (dead plants, woody debris, and litter), and total organic matter across the NMEG. Mean annual precipitation and mean annual temperature are closely correlated across the gradient ($R^2 = 97\%$), allowing for representation of both on the *x*-axis. Lines represent the best-fit equation for carbon storage as a function of mean annual precipitation (all $P < 0.01$; Table S3). NMEG, New Mexico Elevational Gradient.

the two (Figs 2–3). While the site-specific responses differ quantitatively, indicating adaptation to climate, they do not override the dominant effects of climate. As a result, the ratio of daily R_{eco}/GPP increases with temperature and decreases with increasing soil moisture (Fig. 4). These effects play out across the gradient, where elevation serves as a proxy for both decreasing temperature and increasing moisture, such that cool and moist high-elevation ecosystems sequester more carbon annually – and support dramatically more biomass and nonliving organic material – than their low-elevation counterparts (Figs 5–6).

The finding that differential responses of production and respiration to temperature and moisture are manifested across a range of spatio-temporal scales is not an inherently obvious result for several reasons. First, the responses of production and respiration to temperature and moisture are confounded by seasonality (e.g., Yuste *et al*., 2003; Groenendijk *et al*., 2009) and their sensitivities vary across seasons (e.g., Randerson *et al*., 1999; Piao *et al*., 2008; Piao *et al*., 2009). Moreover, the seasonality of precipitation and growth responses varies across ecosystem types (e.g., West *et al*., 2007; Muldavin *et al*., 2008; Méndez-Barroso *et al*., 2009). Nevertheless, both within-site (Figs 2–4) and across site (Figs 4–5) data indicate that – at least on a primary level – differential responses of production and respiration to temperature and moisture persist across spatio-temporal scales. Second, within-site responses to environmental conditions may differ from across-site responses. Ecosystem physiology – the emergent result of individual physiological regulation, acclimatization, adaptation, and community composition – varies strongly across these biomes. However, this is shaped by climate and does not override its dominant effects (Fig. 4). Finally, a number of factors other than temperature and moisture (e.g., soil type, nutrient status, site history) are known to strongly influence the carbon balance of ecosystems (Gifford, 1994; Magnani *et al*., 2007; Piao *et al*., 2009). However, the strong effects of temperature and water availability on NEE observed here indicate that, across the NMEG, these variables play a dominant role in shaping NEE.

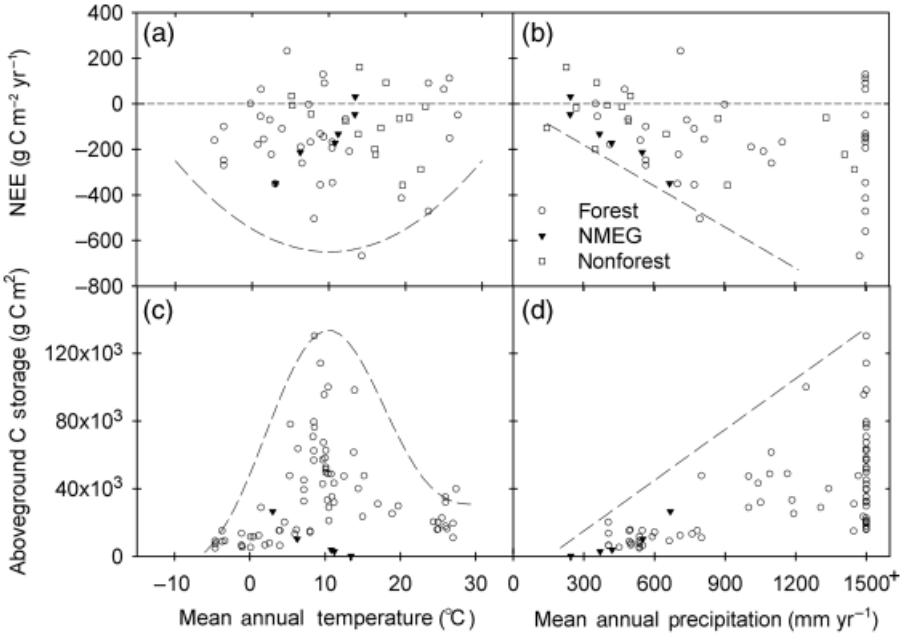

Fig. 7 Variation in NEE and carbon storage across broad climatic gradients for forests, nonforests, and the NMEG sites. Specifically, plotted are annual NEE from undisturbed, unmanaged eddy-covariance sites throughout the world as a function of mean annual temperature (a) and precipitation (b), and total aboveground carbon storage in global forests as a function of temperature (c), and precipitation (d). For NMEG sites, plotted are average annual NEE (2007–2008) and long-term average climate data. Dashed lines represent hypothesized constraints on carbon flux and storage. NEE, net ecosystem exchange; NMEG, New Mexico Elevational Gradient.

Several insights can be obtained by comparing NMEG data to global NEE estimates for other unmanaged ecosystems free of recent disturbance (Fig. 7a–b) and a global forest biomass dataset (Fig. 7c–d). With respect to MAT, sites in the NMEG are not unusual in terms of NEE (Fig. 7a) or biomass storage (Fig. 7c). Our low-elevation sites take up and store relatively little carbon compared with other sites with similar MAT, whereas the high-elevation sites are closer to the apparent limits of NEE or biomass storage at their MAT. This suggests that carbon uptake and storage in the lower elevation sites are strongly limited by water stress, and this is supported by comparison of NMEG sites on a global scale with respect to MAP. The NMEG sites fall along what appears to be a lower limit to NEE as a function of increasing MAP (Fig. 7b), indicating that these sites are sequestering about as much carbon as is possible given their MAP. With regards to biomass storage, the NMEG sites are somewhat below the upper limit of potential biomass storage at a given MAP – possibly because the stress of high temperatures makes it more difficult to accumulate large carbon stocks.

Beyond the NMEG, differential responses of GPP and R_{eco} to temperature and precipitation may help to explain observed global patterns in NEE and biomass storage (e.g., Fig. 7). If the mechanisms described here can be generalized to global scales (e.g., Allen *et al*., 2005), 'steady-state' ecosystems in hot climates should be less likely to act as strong carbon sinks (but see Anderson *et al*. (2006) regarding aggrading forests), and potential sink strength should increase with MAP. Global and regional patterns in NEE of undisturbed, unmanaged ecosystems suggest that this may be the case. In particular, while carbon uptake by ecosystems appears to increase with temperature from high- to mid-latitudes (Fig. 7a; Valentini *et al*., 2000; Magnani *et al*., 2007; Gough *et al*., 2009; Yuan *et al*., 2009), indicating temperature limitation at colder temperatures, this increase does not appear to persist from mid- to low-latitudes (Fig. 7a; e.g., Luyssaert *et al*., 2007). Likewise, the lowest observed annual R_{eco}/GPP ratios are found at intermediate MAT's (Luyssaert *et al*., 2007). With respect to precipitation, other analyses confirm our finding that NEE decreases with increasing precipitation across MAP's of $<1000\,mm\,yr^{-1}$ (e.g., Luyssaert *et al*., 2007). Thus, MAT and MAP may set broad climatic constraints on NEE, while other factors (e.g., disturbance, stand age, N decomposition, CO_2 fertilization, soils) drive the observed substantial variation in NEE within any given climatic region (Gifford, 1994; Magnani *et al*., 2007; Piao *et al*., 2009). Moreover, regional to global patterns in forest biomass (Fig. 7c–d; Keith

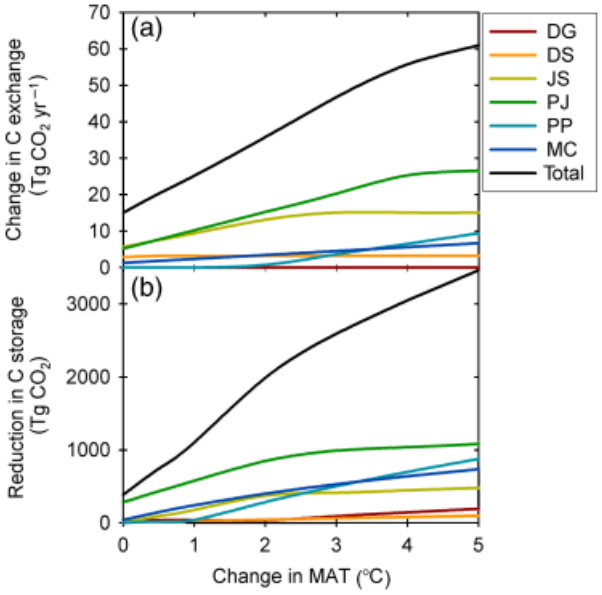

Fig. 8 Predicted changes to the New Mexico terrestrial ecosystem carbon balance as a function of increase in mean annual temperature (MAT): (a) changes in annual ecosystem–atmosphere CO_2 exchange, as predicted based on the relationship between NEE and MAT (Fig. 5; Table S3); (b) potential CO_2 release due to reduced carbon storage capacity, as predicted based on the relationship between total aboveground carbon storage and MAT (Fig. 6d; Table S3). Shown are projected totals for each biome type (predicted change × biome area; Table 1) and the total for all six biome types (representing 57% of the area in NM). Nonzero intercepts reflect discrepancies between measured and predicted values (Figs 5a and 6d). DG, desert grassland; DS, desert shrubland; JS, juniper savannah; PJ, piñon-juniper woodland; PP, ponderosa pine forest; NEE, NEE, net ecosystem exchange.

et al., 2009) and soil organic carbon (e.g., Jobbágy & Jackson, 2000; Allen *et al*., 2005; Meier & Leuschner, 2009) support the idea that ecosystems in moist, temperate climates can accumulate and store the largest amounts of carbon. Data from both the NMEG and global sites indicate that carbon storage may often mirror NEE (Figs 5–7), being the product of NEE integrated over long time scales.

Because the NMEG sites are representative of their biome types (Fig. 1), the climate-dependencies of carbon flux and storage observed here may be used to make first-order estimates of the potential effects of climate change on the carbon balance of much of New Mexico's land area (57%; Fig. 1). Hotter and drier conditions are likely to result in an increasing advantage of respiration relative to GPP on spatio-temporal scales ranging from day-to-day variation within sites (Figs 2–4) to across-site variation in annual R_{eco}/GPP (Table S3). This will result in a reduction of annual carbon sequestration across the elevational gradient; our results predict that NEE would be reduced by 33 g C m^{-2} yr^{-1} for every 1 °C increase in MAT (Fig. 5a). Multiplying aerial coverage of each ecosystem type by predicted changes for each ecosystem type (i.e., difference between 2007 and 2008 mean and predicted NEE at the new temperature, with any predicted NEE > 0 assumed 0) yields the prediction that a 2 °C increase in MAT (predicted for 2025; Christensen *et al*., 2007) would reduce carbon sequestration by these New Mexico ecosystems by 36 Tg CO_2 yr^{-1}, while a 4 °C increase (predicted for end of the century; Christensen *et al*., 2007) would reduce carbon sequestration by 56 Tg CO_2 yr^{-1} (Fig. 8a). Eventually, when the total carbon storage of ecosystems equilibrates to the new climatic conditions, there will be a net loss of foliage, living biomass, detritus, and soil organic carbon (Fig. 6), with corresponding CO_2 release. Extrapolation of the projected loss of total aboveground and soil (top 10 cm only) carbon storage (Fig. 6d–e) to the state level predicts substantial CO_2 release as the carbon storage capacity of these ecosystems is reduced (Fig. 8b). Specifically, a 2 °C increase in MAT would imply a net release of 2 Gt CO_2, while a 4 °C increase would imply a release of 3 Gt CO_2, which exceeds a year's worth of US transportation emissions (US EPA, 2010). These projections assume that (1) future climates will resemble the current climate at a given MAT (e.g., that the MAT–MAP relationship will hold constant, that seasonal patterns in MAT and MAP will remain the same, and that the size distribution of precipitation pulses will remain the same); (2) the carbon-climate relationships observed here are generalizable to future climatic conditions; and (3) ecosystems will equilibrate to the new conditions within the time frame of interest. As these assumptions are likely to be violated, our projections (Fig. 8) should be viewed as rough approximations.

There are several mechanisms by which reduced carbon sequestration and storage may occur – and, indeed, is already occurring throughout the southwest. First, foliage and total living biomass may be reduced by plant mortality through drought and heat stress – either directly through carbon or water stress or indirectly by making trees more susceptible to parasites and disease (e.g., Adams *et al*., 2009; Breshears *et al*., 2009; Allen *et al*., 2010). Recently, there was widespread die-off of piñon pines throughout the southwest caused by drought and associated bark beetle infestations (Breshears *et al*., 2005; Breshears *et al*., 2009). Trees in other southwest biomes (Gitlin *et al*., 2006) and western North America in general (van Mantgem *et al*., 2009) are also experiencing stress and increased mortality. These observations, together with numerous similar cases worldwide, raise concern that drought and heat stress associated with climate change may trigger widespread

forest mortality (Allen *et al*., 2010). In addition, nonliving carbon pools will also be subject to loss under altered climate conditions. Although these may be temporarily augmented by tree mortality, a long-term reduction in production inputs under drought stress (Reichstein *et al*., 2002; Muldavin *et al*., 2008; Schwalm *et al*., 2009) – together with a shift in the balance between respiration and production (Figs. 2–4; Reichstein *et al*., 2002; Arnone *et al*., 2008; Schwalm *et al*., 2009) – will tend to reduce the storage of nonliving organic matter.

Moreover, drought conditions will make these ecosystems – particularly the high elevation sites with high fuel loads – particularly vulnerable to fire. In the Jemez Mountains, where the two highest elevation sites are located, historic fires have tended to occur in drought years (Touchan *et al*., 1996; Swetnam & Betancourt, 1998), and there is evidence that warmer and drier conditions associated with climate change are already increasing forest fire activity in western United States forests (Westerling *et al*., 2006). Fires would trigger substantial carbon release – either immediately (during the burn) or eventually (as vegetation killed by the burn decomposes). Subsequently, the communities that establish after disturbance would, presumably, differ from the former communities (Turner & Romme, 1994), having reduced biomass consistent with the new climatic conditions.

Thus, the capacity of New Mexico ecosystems to store and sequester carbon is likely to be reduced under the projected hotter and drier conditions. As the NMEG is at least qualitatively similar to other elevational gradients in semiarid regions (Whittaker & Niering, 1975; Conant *et al*., 1998), such changes are likely to occur in semiarid ecosystems worldwide. While it is unlikely that these changes will occur in any regular or predictable manner, and while further research will be necessary to understand more specifically how climate sensitivity varies across sites and seasons, the observed climatic dependence of carbon flux and storage strongly implies that – on average – climate change will trigger substantial carbon release from southwest ecosystems and reduce their sink strength. Reduced carbon sequestration, reduced organic matter storage, and increased probability of disturbance will all reduce the value of these ecosystems' greenhouse gas regulation services (Anderson-Teixeira & DeLucia, 2010) and act as a positive feedback to climate change.

Acknowledgements

We gratefully acknowledge Rosemary Pendelton, Andrew Hawk, Shaila Shodean, Dena Smith, and Narlan Teixeira for field work assistance. Thank you to Bob Parmenter and the Valles Caldera National Preserve, Deer Canyon Preserve, LeRoy Humphries and Paul Gardner (7-Up 7-Down Ranch), and the Sevilleta LTER for giving us permission to work on their property. We also want to acknowledge Eric Small, Shirley Kurc, James Cleverly, Jim Thibault, and Cliff Dahm, who originally established the tower sites at the Sevilleta, and Paul Brooks and John Petti, who established the tower sites in the Valles Caldera. Thanks also to Nate McDowell and Doug Moore for providing allometry data, Robert Sinsabaugh and Tierney Adamson for soil organic matter data, Tilden Meyers and Walter Oechel for permission to include unpublished NEE estimates in Fig. 7, and to Marcelo Zeri for helpful discussion. This research was funded by a grant to M. E. L. from the US Forest Service, Rocky Mountain Research Station and financial and infrastructure support to M. E. L. from the National Science Foundation NM-EPSCoR Hydrology Program, National Science Foundation Science and Technology Center for the Sustainability of Semi-Arid Hydrology and Riparian Areas (SAHRA), Sevilleta Long Term Ecological Research and the University of New Mexico. Some allometry datasets were provided by the Sevilleta Long Term Ecological Research (LTER) Program. Significant funding for collection of these data was provided by the National Science Foundation Long Term Ecological Research program (NSF Grant numbers BSR 88-11906, DEB 9411976, DEB 0080529, and DEB 0217774).

References

Adams HD, Guardiola-Claramonte M, Barron-Gafford GA *et al*. (2009) Temperature sensitivity of drought-induced tree mortality portends increased regional die-off under global-change-type drought. *Proceedings of the National Academy of Sciences*, **106**, 7063–7066.

Allen AP, Gillooly JF, Brown JH (2005) Linking the global carbon cycle to individual metabolism. *Functional Ecology*, **19**, 202–213.

Allen AP, Pockman WT, Restrepo C, Milne BT (2008) Allometry, growth and population regulation of the desert shrub *Larrea tridentata*. *Functional Ecology*, **22**, 197–204.

Allen CD, Macalady AK, Chenchouni H *et al*. (2010) A global overview of drought and heat-induced tree mortality reveals emerging climate change risks for forests. *Forest Ecology and Management*, **259**, 660–684.

AmeriFlux Network. *Gap-Filled & Adjusted Data Files with GEP & Re Estimates*. AmeriFlux Network. Available at http://public.ornl.gov/ameriflux/dataproducts.shtml

Anderson-Teixeira KJ, DeLucia EH (2010) The greenhouse gas value of ecosystems. *Global Change Biology*, doi: 10.1111/j.1365-2486.2010.02220.x.

Anderson KJ, Allen AP, Gillooly JF, Brown JH (2006) Temperature-dependence of biomass accumulation rates during secondary succession. *Ecology Letters*, **9**, 673–682.

Anderson-Teixeira KJ, Vitousek PM, Brown JH (2008) Amplified temperature dependence in ecosystems developing on the lava flows of Mauna Loa, Hawai'i. *Proceedings of the National Academy of Sciences*, **105**, 228–233.

Arnone JA III, Verburg PSJ, Johnson DW *et al*. (2008) Prolonged suppression of ecosystem carbon dioxide uptake after an anomalously warm year. *Nature*, **455**, 383–386.

Atkin OK, Macherel D (2009) The crucial role of plant mitochondria in orchestrating drought tolerance. *Annals of Botany*, **103**, 581–597.

Atkin OK, Scheurwater I, Pons TL (2007) Respiration as a percentage of daily photosynthesis in whole plants is homeostatic at moderate, but not high, growth temperatures. *New Phytologist*, **174**, 367–380.

Atkin OK, Tjoelker MG (2003) Thermal acclimation and the dynamic response of plant respiration to temperature. *Trends in Plant Science*, **8**, 343–351.

Austin AT (2002) Differential effects of precipitation on production and decomposition along a rainfall gradient in Hawaii. *Ecology*, **83**, 328–338.

Beringer J, Hutley LB, Tapper NJ, Cernusak LA (2007) Savanna fires and their impact on net ecosystem productivity in North Australia. *Global Change Biology*, **13**, 990–1004.

Breshears D, Myers O, Meyer CW *et al*. (2009) Tree die-off in response to global change-type drought: mortality insights from a decade of plant water potential measurements. *Frontiers in Ecology and the Environment*, **7**, 185–189.

Breshears DD, Cobb NS, Rich PM *et al*. (2005) Regional vegetation die-off in response to global-change-type drought. *Proceedings of the National Academy of Sciences*, **102**, 15144–15148.

Christensen J, Hewitson B, Busuioc A *et al*. (2007) Regional climate projections. In: *Climate Change 2007: The Physical Science Basis. Contribution of Working Group I to the Fourth Assessment Report of the Intergovernmental Panel on Climate Change* (eds Solomon S, Qin D, Manning M, Chen Z, Marquis M, Averyt KB, Tignor M, Miller HL), Cambridge University Press Cambridge, UK, New York, NY, USA.

Ciais P, Reichstein M, Viovy N *et al*. (2005) Europe-wide reduction in primary productivity caused by the heat and drought in 2003. *Nature*, **437**, 529–533.

Clark KL, Gholz HL, Moncrieff JB, Cropley F, Loescher HW (1999) Environmental controls over net exchanges of carbon dioxide from contrasting Florida ecosystems. *Ecological Applications*, **9**, 936–948.

Conant RT, Klopatek JM, Malin RC, Klopatek CC (1998) Carbon pools and fluxes along an environmental gradient in northern Arizona. *Biogeochemistry*, **43**, 43–61.

DeLucia EH, Drake J, Thomas RB, Gonzalez-Meler MA (2007) Forest carbon use efficiency: is respiration a constant fraction of gross primary production? *Global Change Biology*, **13**, 1157–1167.

Dick-Peddie W (1999) *New Mexico Vegetation: Past, Present, and Future*. University of New Mexico Press, Albuquerque, NM, USA.

Dugas WA, Heuer ML, Mayeux HS (1999) Carbon dioxide fluxes over bermudagrass, native prairie, and sorghum. *Agricultural and Forest Meteorology*, **93**, 121–139.

Enquist B, Niklas K (2002) Global allocation rules for patterns of biomass partitioning in seed plants. *Science*, **295**, 1517–1520.

Falge E, Aubinet M, Bakwin P *et al*. (2005) *FLUXNET Marconi Conference Gap-Filled Flux and Meteorology Data, 1992–2000*. Oak Ridge National Laboratory Distributed Active Archive Center, Oak Ridge, TN, USA.

Falge E, Baldocchi D, Olson R *et al*. (2001) Gap filling strategies for defensible annual sums of net ecosystem exchange. *Agricultural and Forest Meteorology*, **107**, 43–69.

Field CB, Lobell DB, Peters HA, Chiariello NR (2007) Feedbacks of terrestrial ecosystems to climate change. *Annual Review of Environment and Resources*, **32**, 1–29.

Flanagan LB, Wever LA, Carlson PJ (2002) Seasonal and interannual variation in carbon dioxide exchange and carbon balance in a northern temperate grassland. *Global Change Biology*, **8**, 599–615.

Foster RC (1988) Microenvironments of soil microorganisms. *Biology and Fertility of Soils*, **6**, 189–203.

Gifford R (1994) The global carbon cycle: a viewpoint on the missing sink. *Functional Plant Biology*, **21**, 1–15.

Gilmanov TG, Svejcar TJ, Johnson DA, Angell RF, Saliendra NZ, Wylie BK (2006) Long-term dynamics of production, respiration, and net CO_2 exchange in two sagebrush-steppe ecosystems. *Rangeland Ecology & Management*, **59**, 585–599.

Gilmanov TG, Tieszen LLUSDA A *et al*. (2005) Integration of CO_2 flux and remotely-sensed data for primary production and ecosystem respiration analyses in the Northern Great Plains: potential for quantitative spatial extrapolation. *Global Ecology & Biogeography*, **14**, 271–292.

Gitlin AR, Sthultz CM, Bowker MA *et al*. (2006) Mortality gradients within and among dominant plant populations as barometers of ecosystem change during extreme drought. *Conservation Biology*, **20**, 1477–1486.

Gough CM, Flower CE, Vogel CS, Dragoni D, Curtis PS (2009) Whole-ecosystem labile carbon production in a north temperate deciduous forest. *Agricultural and Forest Meteorology*, **149**, 1531–1540.

Grier C, Elliot K, McCullough D (1992) Biomass distribution and productivity of *Pinus edulis-Juniperus monosperma* woodlands of north-central Arizona. *Forest Ecology and Management*, **50**, 331–350.

Groenendijk M, van der Molen MK, Dolman AJ (2009) Seasonal variation in ecosystem parameters derived from FLUXNET data. *Biogeosciences Discuss*, **6**, 2863–2912. Available at http://www.biogeosciences-discuss.net/6/2863/2009/

Hogberg P, Nordgren A, Buchmann N, Taylor AFS, Ekblad A, Hogberg MN, Nyberg G, Ottosson-Lofvenius M, Read DJ (2001) Large-scale forest girdling shows that current photosynthesis drives soil respiration. *Nature*, **411**, 789–792.

Hollinger DY, Richardson AD (2005) Uncertainty in eddy covariance measurements and its application to physiological models. *Tree Physiol*, **25**, 873–885.

Hu J, Moore DJP, Burns SP, Monson RK (2010) Longer growing seasons lead to less carbon sequestration by a subalpine forest. *Global Change Biology*, **16**, 771–783.

Hughes MK, Diaz HF (2008) Climate variability and change in the drylands of western North America. *Global and Planetary Change*, **64**, 111–118.

Huxman TE, Smith MD, Fay PA *et al*. (2004a) Convergence across biomes to a common rain-use efficiency. *Nature*, **429**, 651–654.

Huxman TE, Snyder KA, Tissue D *et al*. (2004b) Precipitation pulses and carbon fluxes in semiarid and arid ecosystems. *Oecologia*, **141**, 254–268.

Inglima I, Alberti G, Bertolini T *et al*. (2009) Precipitation pulses enhance respiration of Mediterranean ecosystems: the balance between organic and inorganic components of increased soil CO_2 efflux. *Global Change Biology*, **15**, 1289–1301.

IPCC (2007) *Climate Change 2007: Impacts, Adaptation and Vulnerability. Contribution of Working Group II to the Fourth Assessment Report of the Intergovernmental Panel on Climate Change*. IPCC, Cambridge, UK.

Jenerette G, Scott RL, Huxman TE (2008) Whole ecosystem metabolic pulses following precipitation events. *Functional Ecology*, **22**, 924–930.

Jenkins JC, Chojnacky DC, Heath LS, Birdsey RA (2003) National-scale biomass estimators for United States tree species. *Forest Science*, **49**, 12–35.

Jobbágy EG, Jackson RB (2000) Global controls of forest line elevation in the northern and southern hemispheres. *Global Ecology and Biogeography*, **9**, 253–268.

Jornada LTER (2007) *Annual Aboveground Net Primary Production, Summary (ANNPROD.DSD)*. Jornada LTER, New Mexico State University, Las Cruces, NM Available at http://www.nmsu.edu/datacat.php

Keith H, Mackey BG, Lindenmayer DB (2009) Re-evaluation of forest biomass carbon stocks and lessons from the world's most carbon-dense forests. *Proceedings of the National Academy of Sciences*, **106**, 11635–11640.

King AW, Gunderson CA, Post WM, Weston DJ, Wullschleger SD (2006) Plant respiration in a warmer world. *Science*, **312**, 536–537.

Kirschbaum MUF (1995) The temperature dependence of soil organic matter decomposition, and the effect of global warming on soil organic C storage. *Soil Biology & Biochemistry*, **27**, 753–760.

Law BE, Falge E, Gu L *et al*. (2002) Environmental controls over carbon dioxide and water vapor exchange of terrestrial vegetation. *Agricultural and Forest Meteorology*, **113**, 97–120.

Leung LR, Qian Y, Bian X, Washington WM, Han J, Roads JO (2004) Mid-century ensemble regional climate change scenarios for the western United States. *Climatic Change*, **62**, 75–113.

Leuning R, Cleugh HA, Zegelin SJ, Hughes D (2005) Carbon and water fluxes over a temperate Eucalyptus forest and a tropical wet/dry savanna in Australia: measurements and comparison with MODIS remote sensing estimates. *Agricultural and Forest Meteorology*, **129**, 151–173.

Litton CM, Raich JW, Ryan MG (2007) Carbon allocation in forest ecosystems. *Global Change Biology*, **13**, 2089–2109.

Luyssaert S, Inglima I, Jung M *et al*. (2007) CO_2 balance of boreal, temperate, and tropical forests derived from a global database. *Global Change Biology*, **13**, 2509–2537.

Magnani F, Mencuccini M, Borghetti M *et al*. (2007) The human footprint in the carbon cycle of temperate and boreal forests. *Nature*, **447**, 849–851.

Massman WJ (2000) A simple method for estimating frequency response corrections for eddy covariance systems. *Agricultural and Forest Meteorology*, **104**, 185–198.

McDowell NG, White S, Pockman WT (2008) Transpiration and stomatal conductance across a steep climate gradient in the southern Rocky Mountains. *Ecohydrology*, **1**, 193–204.

Meier IC, Leuschner C (2009) Variation of soil and biomass carbon pools in beech forests across a precipitation gradient. *Global Change Biology*, **16**, 1035–1045.

Méndez-Barroso LA, Vivoni ER, Watts CJ, Rodríguez JC (2009) Seasonal and interannual relations between precipitation, surface soil moisture and vegetation dynamics in the North American monsoon region. *Journal of Hydrology*, **377**, 59–70.

Monson RK, Lipson DL, Burns SP, Turnipseed AA, Delany AC, Williams MW, Schmidt SK (2006) Winter forest soil respiration controlled by climate and microbial community composition. *Nature*, **439**, 711–714.

Muldavin E (2004). *Sevilleta LTER Fertilizer NPP Study Dataset*. Sevilleta Long Term Ecological Research Site Database: SEV155, Albuquerque, NM. Available at http://sev.lternet.edu/project_details.php?id=SEV155 (accessed 28 July 2005).

Muldavin E, Moore D, Collins S, Wetherill K, Lightfoot D (2008) Aboveground net primary production dynamics in a northern chihuahuan desert ecosystem. *Oecologia*, **155**, 123–132.

National Resources Conservation Service (2009) *Web Soil Servey*. USDA. Available at http://websoilsurvey.nrcs.usda.gov/app/ (accessed May 2010).

Novick K, Stoy P, Katul G, Ellsworth DS, Siqueira M, Juang J, Oren R (2004) Carbon dioxide and water vapor exchange in a warm temperate grassland. *Oecologia*, **138**, 259–274.

Oak Ridge National Laboratory Distributed Active Archive Center (ORNL DAAC). 2009 *MODIS Subsetted Land Products, Collection 5*. ORNL DAAC, Oak Ridge, TN, USA Available at http://www.daac.ornl.gov/MODIS/modis.html (accessed July 2007).

Orchard VA, Cook F (1983) Relationship between soil respiration and soil moisture. *Soil Biology and Biochemistry*, **15**, 447–453.

Piao S, Ciais P, Friedlingstein P *et al*. (2008) Net carbon dioxide losses of northern ecosystems in response to autumn warming. *Nature*, **451**, 49–52.

Piao S, Friedlingstein P, Ciais P, Peylin P, Zhu B, Reichstein M (2009) Footprint of temperature changes in the temperate and boreal forest carbon balance. *Geophysical Research Letter*, **36**, L07404, doi: 10.1029/2009GL037381.

Portmann RW, Solomon S, Hegerl GC (2009) Spatial and seasonal patterns in climate change, temperatures, and precipitation across the United States. *Proceedings of the National Academy of Sciences*, **106**, 7324–7329.

Randerson JT, Field CB, Fung IY, Tans PP (1999) Increases in early season ecosystem uptake explain recent changes in the seasonal cycle of atmospheric CO_2 at high northern latitudes. *Geophysical Research Letter*, **26**, 2765–2769.

Reichstein M, Falge E, Baldocchi D *et al.* (2005) On the separation of net ecosystem exchange into assimilation and ecosystem respiration: review and improved algorithm. *Global Change Biology*, **11**, 1424–1439.

Reichstein M, Papale D, Valentini R *et al.* (2007) Determinants of terrestrial ecosystem carbon balance inferred from European eddy covariance flux sites. *Geophysical Research Letters*, **34**, L01402, doi: 10.1029/2006GL027880.

Reichstein M, Tenhunen JD, Roupsard O *et al.* (2002) Severe drought effects on ecosystem CO_2 and H_2O fluxes at three mediterranean evergreen sites: revision of current hypotheses? *Global Change Biology*, **8**, 999–1017.

Risser P, Birney E, Blocker S, May W (1981) *The True Prairie Ecosystem*. Hutchingson Ross Publishing Company, Stroudsburg, PA.

Rustad L, Campbell JGCTE-NEWS (2001) A meta-analysis of the response of soil respiration, net nitrogen mineralization, and aboveground plant growth to experimental ecosystem warming. *Oecologia*, **126**, 543–562.

Ryan MG, Law BE (2005) Interpreting, measuring, and modeling soil respiration. *Biogeochemistry*, **73**, 3–27.

Santos AJB, Silva GTDA, Miranda HS, Miranda AC, Lloyd J (2003) Effects of fire on surface carbon, energy and water vapour fluxes over campo sujo savanna in central Brazil. *Functional Ecology*, **17**, 711–719.

Schwalm CR, Williams CA, Schaefer K *et al.* (2009) Assimilation exceeds respiration sensitivity to drought: a FLUXNET synthesis. *Global Change Biology*, **16**, 657–670.

Seager R, Ting MF, Held I *et al.* (2007) Model projections of an imminent transition to a more arid climate in southwestern North America. *Science*, **316**, 1181–1184.

Sevilleta LTER (2007) *The Plant Line-Intercept Transects (SEV004)*. Sevilleta LTER, University of New Mexico, Albuquerque, NM, USA.

Shaver GR, Canadell J, Chapin FS III (2000) Global warming and terrestrial ecosystems: a conceptual framework for analysis. *Bioscience*, **50**, 871–882.

Stoy PC, Katul GG, Siqueira MBS *et al.* (2008) Role of vegetation in determining carbon sequestration along ecological succession in the southeastern united states. *Global Change Biology*, **14**, 1409–1427.

Suyker AE, Verma SB, Burba GG (2003) Interannual variability in net CO_2 exchange of a native tallgrass prairie. *Global Change Biology*, **9**, 255–265.

Svejcar T, Angell R, Bradford JA *et al.* (2008) Carbon fluxes on north American rangelands. *Rangeland Ecology & Management*, **61**, 465–474.

Swetnam TW, Betancourt JL (1998) Mesoscale disturbance and ecological response to decadal climatic variability in the American southwest. *Journal of Climate*, **11**, 3128–3147.

Touchan R, Allen CD, Swetnam TW (1996) *Fire History and Climatic Patterns in Ponderosa Pine and Mixed-Conifer Forests of the Jemez Mountains, Northern New Mexico*. USDA Forest Service, Rocky Mountain Forest and Range Experiment Station, Fort Collins, CO.

Turner MG, Romme WH (1994) Landscape dynamics in crown fire ecosystems. *Landscape Ecology*, **9**, 59–77.

US EPA (2010) *Inventory of U.S. Greenhouse Gas Emissions and Sinks: 1990–2008 (EPA 430-R-10-006)*. U.S. Environmental Protection Agency, Washington, DC.

USDA Forest Service (2007) *Forest Inventory and Analysis Database*. USDA.

Valentini R, Gamon JA, Field CB (1995) Ecosystem gas exchange in a California grassland: seasonal patterns and implications for scaling. *Ecology*, **76**, 1940–1952.

Valentini R, Matteucci G, Dolman AJ *et al.* (2000) Respiration as the main determinant of carbon balance in European forests. *Nature*, **404**, 861–865.

van Mantgem PJ, Stephenson NL, Byrne JC *et al.* (2009) Widespread increase of tree mortality rates in the western united states. *Science*, **323**, 521–524.

Veenendaal EM, Kolle O, Lloyd J (2004) Seasonal variation in energy fluxes and carbon dioxide exchange for a broad-leaved semi-arid savanna (Mopane woodland) in Southern Africa. *Global Change Biology*, **10**, 318–328.

Webb EK, Pearman GI, Leuning R (1980) Correction of flux measurements for density effects due to heat and water vapour transfer. *Quarterly Journal of the Royal Meteorological Society*, **106**, 85–100.

Weiss JL, Castro CL, Overpeck JT (2009) Distinguishing pronounced droughts in the southwestern United States: seasonality and effects of warmer temperatures. *Journal of Climate*, **22**, 5918–5932.

West A, Hultine K, Burtch K, Ehleringer J (2007) Seasonal variations in moisture use in a piñon–juniper woodland. *Oecologia*, **153**, 787–798.

West G, Brown J, Enquist B (1999) A general model for the structure and allometry of plant vascular systems. *Nature*, **400**, 664–667.

Westerling AL, Hidalgo HG, Cayan DR, Swetnam TW (2006) Warming and earlier spring increase western U.S. forest wildfire activity. *Science*, **313**, 940–943.

Whittaker R, Niering W (1975) Vegetation of the Santa Catalina Mountains, Arizona. V. biomass, production, and diversity along the elevation gradient. *Ecology*, **56**, 771–790.

Wohlfahrt G, Fenstermaker LF, John A, Arnone I (2008) Large annual net ecosystem CO_2 uptake of a Mojave desert ecosystem. *Global Change Biology*, **14**, 1475–1487.

Yuan W, Lou Y, Richardson AD *et al.* (2009) Latitudinal patterns of magnitude and interannual variability in net ecosystem exchange regulated by biological and environmental variables. *Global Change Biology*, **15**, 2905–2920.

Yuste JC, Janssens IA, Carrara A, Meiresonne L, Ceulemans R (2003) Interactive effects of temperature and precipitation on soil respiration in a temperate maritime pine forest. *Tree Physiology*, **23**, 1263–1270.

Supporting Information

Additional Supporting Information may be found in the online version of this article:

Table S1. Allometric relationships used to estimate biomass across the NMEG. Here, M_{ag} is aboveground biomass (g dry), M_f is foliage biomass (g dry), h is height (m), *dbh* is diameter at breast height (cm), *rcd* is root crown diameter as defined in Grier *et al.* (1992), and v is volume (m^3; calculated as product of height and two perpendicular diameters). Coefficients of some allometries are modified from the original in order to express all equations in common units.

Table S2. Carbon storage ($g\,C\,m^{-2}$) in aboveground organic matter pools across the NMEG. Values presented are mean (1 s.e.).

Table S3. Best-fit relationships between *NEE* ($g\,C\,m^{-2}\,yr^{-1}$), and biomass pools ($g\,C\,m^{-2}$) to climate variables: measured annual precipitation and temperature (NEE) or long-term average mean annual precipitation (MAP; $mm\,yr^{-1}$) and mean annual temperature (MAT; °C) (biomass pools). Numbers in parentheses represent 1 s.e. of parameter estimate.

Please note: Wiley-Blackwell are not responsible for the content or functionality of any supporting materials supplied by the authors. Any queries (other than missing material) should be directed to the corresponding author for the article.